

**SYNTHESIS, CHARACTERIZATION AND MESOMORPHIC PROPERTIES  
OF SYMMETRIC AND NON-SYMMETRIC ISOFLAVONE OLIGOMERS**

**by**

**CHAN TZE NEE**

**Thesis submitted in fulfillment of the requirements  
for the degree of  
Master of Science**

**May 2012**

## ACKNOWLEDGEMENT

I wish to take this opportunity to thank my main supervisor, Professor Yeap Guan Yeow for his teaching and invaluable guidance to my research throughout the period of my candidature. Also, I would like to express my appreciation to my co-supervisor, Dr Yam Wan Sinn for giving me advice and assistance generously. I wish to thank the Dean and staff of School of Chemical Sciences for providing me with the research facilities. My gratitude also goes to the Dean of Institute of Postgraduate Studies for giving me a chance to be enrolled as a MSc student at Universiti Sains Malaysia and the scholarship (USM Fellowship) provided throughout the period of my study.

I wish to thank Professor Ewa Gorecka from Warsaw University, Poland, who is also my field supervisor, for the assistance in X-ray analysis and sharing her expertise in liquid crystal research with me. I would also like to express my sincere appreciation to Professor Corrie T. Imrie and Dr Lu Zhi Bao from University of Aberdeen, Scotland, Associate Professor Daisuke Takeuchi from Tokyo Institute of Technology, Professor Masato M. Ito from Soka University, Japan and Miss Karolina Madrak from Warsaw University, Poland for some analytical measurements which could not be carried out in USM owing to the lack of instruments. I am also grateful to my laboratory mates for sharing their knowledge with me and providing me with great assistances in many aspects at the workplace.

To my family and friends, I wish to convey my best regards and gratitude for their support all this while.

## TABLE OF CONTENTS

<b>ACKNOWLEDGEMENT</b> .....	ii
<b>TABLE OF CONTENTS</b> .....	iii
<b>LIST OF TABLES</b> .....	viii
<b>LIST OF FIGURES</b> .....	xi
<b>LIST OF ABBREVIATION</b> .....	xix
<b>ABSTRAK</b> .....	xxii
<b>ABSTRACT</b> .....	xxiv
<b>1.0 INTRODUCTION</b> .....	1
1.1 Liquid crystals .....	1
1.2 Types of liquid crystals .....	2
1.3 Mesophases .....	2
1.3.1 Nematic phase .....	2
1.3.1.1 Cholesteric phase .....	2
1.3.2 Smectic phase .....	3
1.3.2.1 Smectic A phase .....	3
1.3.2.2 Smectic C phase .....	3
1.3.2.3 Chiral smectic phase .....	4
1.4 Liquid crystal oligomers .....	4
1.4.1 Liquid crystal dimers .....	5
1.4.2 Liquid crystal trimers .....	5
1.5 Structure-property relationship of liquid crystal oligomers .....	6
1.5.1 Phase behaviour in liquid crystal oligomers .....	6
1.5.2 Layer arrangement of smectic phase in liquid crystal oligomers .....	7

1.5.3	Odd-even effect in liquid crystal oligomers.....	9
1.5.4	Chirality effect on liquid crystalline properties of oligomers ...	11
1.6	Liquid crystals oligomers incorporating isoflavone moiety .....	12
1.7	Research objectives.....	13
<b>2.0</b>	<b>EXPERIMENTAL</b> .....	14
2.1	Chemicals.....	14
2.2	Instruments.....	14
2.3	Synthesis .....	16
2.3.1	Preparation of 7-[{4-[4'-(( <i>S</i> )-2"-methylbutyloxy)carbonylphenyl]phenoxy}alkyloxy]-3-(4'-decyloxyphenyl)-4 <i>H</i> -1-benzopyran-4-ones, <b>BP-n-I</b> (n = 3-12)	16
2.3.1.1	Synthesis of ( <i>S</i> )-(-)-2-methylbutyl-4'-(4"-hydroxyphenyl)benzoate, <b>HBP</b> .....	18
2.3.1.2	Synthesis of 4-decyloxyphenylacetic acid, <b>DPA</b> .....	18
2.3.1.3	Synthesis of 7-hydroxy-3-(4'-decyloxyphenyl)-4 <i>H</i> -1-benzopyran-4-one, <b>HDI</b> .....	18
2.3.1.4	Syntheses of 7-(n-bromoalkyloxy)-3-(4'-decyloxyphenyl)-4 <i>H</i> -1-benzopyran-4-ones, <b>Br-n-I</b> (n = 3-12) .....	19
2.3.1.5	Syntheses of 7-[{4-[4'-(( <i>S</i> )-2"-methylbutyloxy)carbonylphenyl]phenoxy}alkyloxy]-3-(4'-decyloxyphenyl)-4 <i>H</i> -1-benzopyran-4-ones, <b>BP-n-I</b> (n = 3-12).....	19
2.3.2	Preparation of 7-[{4-[4'-(( <i>S</i> )-2"-methylbutyloxy)carbonylphenyl]phenoxy}decyloxy]-3-(4'-	

substitutedphenyl)-4 <i>H</i> -1-benzopyran-4-ones, <b>BPI-R</b> (R = H, CH <sub>3</sub> , OCH <sub>3</sub> , F, Cl, Br).....	20
2.3.2.1 Syntheses of 7-hydroxy-3-(4'-substitutedphenyl)-4 <i>H</i> -1-benzopyran-4-ones, <b>HI-R</b> (R = H, CH <sub>3</sub> , OCH <sub>3</sub> , F, Cl, Br).....	21
2.3.2.2 Syntheses of 7-(10-bromodecyloxy)-3-(4'-substitutedphenyl)-4 <i>H</i> -1-benzopyran-4-ones, <b>BrI-R</b> (R = H, CH <sub>3</sub> , OCH <sub>3</sub> , F, Cl, Br).....	21
2.3.2.3 Syntheses of 7-[{4-[4'-(( <i>S</i> )-2"-methylbutyloxy)carbonylphenyl]phenoxy}decyloxy]-3-(4'-substitutedphenyl)-4 <i>H</i> -1-benzopyran-4-ones, <b>BPI-R</b> (R = H, CH <sub>3</sub> , OCH <sub>3</sub> , F, Cl, Br) .....	21
2.3.3 Preparation of 7-[{4-[(4'-methoxyphenyl)diazenyl]phenoxy}alkyloxy]-3-(4'-methoxyphenyl)-4 <i>H</i> -1-benzopyran-4-ones, <b>AB-n-I</b> (n = 3-10)	22
2.3.3.1 Synthesis of 4-[(4'-methoxyphenyl)diazenyl]phenol, <b>HAB</b> .....	23
2.3.3.2 Syntheses of 1-[4-(n-bromoalkyloxy)phenyl]-2-(4'-methoxyphenyl)diazene, <b>AB-n-Br</b> (n = 3-10) .....	23
2.3.3.3 Synthesis of 7-hydroxy-3-(4'-methoxyphenyl)-4 <i>H</i> -1-benzopyran-4-one, <b>HI-OCH<sub>3</sub></b> .....	23
2.3.3.4 Syntheses of 7-[{4-[(4'-methoxyphenyl)diazenyl]phenoxy}alkyloxy]-3-(4'-methoxyphenyl)-4 <i>H</i> -1-benzopyran-4-ones, <b>AB-n-I</b> (n = 3-10) .....	24

2.3.4	Preparation of 1,3-bis{[3-(4'-decyloxyphenyl)-4 <i>H</i> -1-benzopyran-4-one-7-oxy]alkyloxy}benzenes, <b>BI-n-B</b> (n = 3-12)	25
2.3.4.1	Syntheses of 1,3-bis{[3-(4'-decyloxyphenyl)-4 <i>H</i> -1-benzopyran-4-one-7-oxy]alkyloxy}benzenes, <b>BI-n-B</b> (n = 3-12)	26
2.4	Characterization	26
<b>3.0</b>	<b>RESULTS AND DISCUSSION</b>	28
3.1	7-[{4-[4'-(( <i>S</i> )-2"-methylbutyloxy)carbonylphenyl]phenoxy}alkyloxy]-3-(4'-decyloxyphenyl)-4 <i>H</i> -1-benzopyran-4-one, <b>BP-n-I</b>	28
3.1.1	Physical characterization	28
3.1.1.1	Fourier transform infrared spectroscopy (FT-IR)	29
3.1.1.2	Fourier transform nuclear magnetic resonance spectroscopy (FT-NMR)	31
3.1.2	Thermal and optical behaviour	46
3.2	7-[{4-[4'-(( <i>S</i> )-2"-methylbutyloxy)carbonylphenyl]phenoxy}decyloxy]-3-(4'-substitutedphenyl)-4 <i>H</i> -1-benzopyran-4-ones, <b>BPI-R</b>	56
3.2.1	Physical characterization	56
3.2.1.1	Fourier transform infrared spectroscopy (FT-IR)	56
3.2.1.2	Fourier transform nuclear magnetic resonance spectroscopy (FT-NMR)	58
3.2.2	Thermal and optical behaviour	71
3.3	7-[{4-[4'-(4'-methoxyphenyl)diazenyl]phenoxy}alkyloxy]-3-(4'-methoxyphenyl)-4 <i>H</i> -1-benzopyran-4-ones, <b>AB-n-I</b>	77
3.3.1	Physical characterization	77

3.3.1.1	Fourier transform infrared spectroscopy (FT-IR) .....	78
3.3.1.2	Fourier transform nuclear magnetic resonance spectroscopy (FT-NMR) .....	80
3.3.2	Thermal and optical behaviour .....	91
3.4	1,3-bis{[3-(4'-decyloxyphenyl)-4 <i>H</i> -1-benzopyran-4-one-7- oxy]alkyloxy}benzenes, <b>BI-n-B</b> .....	96
3.4.1	Physical characterization.....	96
3.4.1.1	Fourier transform infrared spectroscopy (FT-IR) .....	96
3.4.1.2	Fourier transform nuclear magnetic resonance spectroscopy (FT-NMR) .....	98
3.4.2	Thermal and optical behaviour .....	110
3.5	Structure-property relationship .....	118
<b>4.0</b>	<b>CONCLUSION</b> .....	121
	<b>REFERENCES</b> .....	123
	<b>APPENDICES</b> .....	135
	Appendix A: International publications .....	135
	Appendix B: Papers presented in local conferences .....	136
	Appendix C: FT-NMR spectrum .....	137

## LIST OF TABLES

Table 3.1	Empirical formulas, molecular weights (MW), percentage yields (%) and CHN microanalytical data of <b>BP-n-I</b> .....	28
Table 3.2	Selected FT-IR absorption frequencies, $\nu/\text{cm}^{-1}$ and relative intensities of <b>BP-n-I</b> .....	29
Table 3.3	$^1\text{H}$ -NMR chemical shifts, $\delta/\text{ppm}$ of <b>BP-n-I</b> .....	37
Table 3.4	$^{13}\text{C}$ -NMR chemical shifts, $\delta/\text{ppm}$ of <b>BP-n-I</b> .....	40
Table 3.5	$^1\text{H}$ - $^1\text{H}$ correlations as inferred from 2D COSY experiment for <b>BP-5-I</b>	45
Table 3.6	$^1\text{H}$ - $^{13}\text{C}$ correlations as inferred from the 2D HMQC and HMBC experiments for <b>BP-5-I</b> .....	45
Table 3.7	Phase transition temperatures / $^{\circ}\text{C}$ and enthalpy change values ( $\text{kJmol}^{-1}$ ) of <b>BP-n-I</b> upon heating.....	50
Table 3.8	The SmA* layer spacing(s), $d$ , measured using X-ray diffraction, the estimated all- <i>trans</i> molecular length(s), $L$ , and the corresponding $d/L$ ratios for <b>BP-n-I</b> .....	53
Table 3.9	Empirical formulas, molecular weights (MW), percentage yields (%) and CHN microanalytical data of <b>BPI-R</b> .....	56
Table 3.10	Selected FT-IR absorption frequencies, $\nu/\text{cm}^{-1}$ and relative intensities of <b>BPI-R</b> .....	58
Table 3.11	$^1\text{H}$ -NMR chemical shifts, $\delta/\text{ppm}$ of <b>BPI-R</b> .....	62
Table 3.12	$^{13}\text{C}$ -NMR chemical shifts, $\delta/\text{ppm}$ of <b>BPI-R</b> .....	65
Table 3.13	$^1\text{H}$ - $^1\text{H}$ correlations as inferred from 2D COSY experiment for <b>BPI-Br</b> .....	70



Table 3.14	$^1\text{H}$ - $^{13}\text{C}$ correlations as inferred from the 2D HMQC and HMBC experiments for <b>BPI-Br</b> .....	70
Table 3.15	Phase transition temperatures/ $^{\circ}\text{C}$ and enthalpy change values ( $\text{kJmol}^{-1}$ ) of <b>BPI-R</b> during heating .....	72
Table 3.16	The SmA* layer spacing(s), $d$ , measured using X-ray diffraction, the estimated all- <i>trans</i> molecular length(s), $L$ , and the corresponding $d/L$ ratios for <b>BPI-R</b> .....	74
Table 3.17	Calculated polarizability values for <b>BPI-R</b> .....	76
Table 3.18	Empirical formulas, molecular weights (MW), percentage yields (%) and CHN microanalytical data of <b>AB-n-I</b> .....	77
Table 3.19	Selected FT-IR absorption frequencies, $\text{v/cm}^{-1}$ and relative intensities of <b>AB-n-I</b> .....	78
Table 3.20	$^1\text{H}$ -NMR chemical shifts, $\delta/\text{ppm}$ of <b>AB-n-I</b> .....	83
Table 3.21	$^{13}\text{C}$ -NMR chemical shifts, $\delta/\text{ppm}$ of <b>AB-n-I</b> .....	85
Table 3.22	$^1\text{H}$ - $^1\text{H}$ correlations as inferred from 2D COSY experiment for <b>AB-5-I</b> 90	
Table 3.23	$^1\text{H}$ - $^{13}\text{C}$ correlations as inferred from the 2D HMQC and HMBC experiments for <b>AB-5-I</b> .....	90
Table 3.24	Phase transition temperatures/ $^{\circ}\text{C}$ , enthalpy change values ( $\text{kJmol}^{-1}$ ) and entropy change associated with N-Iso transition of <b>AB-n-I</b> during heating.....	91
Table 3.25	Empirical formulas, molecular weights (MW), percentage yields (%) and CHN microanalytical data of <b>BI-n-B</b> .....	96
Table 3.26	Selected FT-IR absorption frequencies, $\text{v/cm}^{-1}$ and relative intensities of <b>BI-n-B</b> .....	98
Table 3.27	$^1\text{H}$ -NMR chemical shifts, $\delta/\text{ppm}$ of <b>BI-n-B</b> .....	101

Table 3.28	$^{13}\text{C}$ -NMR chemical shifts, $\delta/\text{ppm}$ of <b>BI-n-B</b> .....	104
Table 3.29	$^1\text{H}$ - $^1\text{H}$ correlations as inferred from 2D COSY experiment for <b>BI-4-B</b> .....	109
Table 3.30	$^{13}\text{C}$ - $^1\text{H}$ correlations as inferred from the 2D HMQC and HMBC experiments for <b>BI-4-B</b> .....	109
Table 3.31	Phase transition temperatures / $^{\circ}\text{C}$ and enthalpy change values ( $\text{kJmol}^{-1}$ ) of <b>BI-n-B</b> upon heating.....	113

## LIST OF FIGURES

Figure 1.1	Arrangement of molecules in solid, liquid crystal and liquid .....	1
Figure 1.2	Diagrammatic representation of (a) N and (b) N* phases .....	3
Figure 1.3	Molecular arrangement in (a) SmA and (b) SmC phases .....	4
Figure 1.4	A SmC* material showing the rotation of tilted director from layer to layer forming a helical structure .....	5
Figure 1.5	Diagrammatic representation of SmA arrangements in dimeric liquid crystals, (a) monolayer, (b) intercalated and (c) interdigitated .....	8
Figure 1.6	Diagrammatic representation of dimeric molecules with (a) an odd and (b) an even number of flexible units between two mesogenic moieties .....	9
Figure 1.7	Molecular shapes of the all- <i>trans</i> conformation of trimers containing (a) odd- and (b) even-parity flexible spacers .....	10
Figure 1.8	A general structure of isoflavone (3-phenyl-4 <i>H</i> -1-benzopyran-4-one). 13	
Figure 2.1	Synthetic scheme for the formation of 7-[[4-[4'-(( <i>S</i> )-2'-methylbutyloxy)carbonylphenyl]phenoxy}alkyloxy]-3-(4'-decyloxyphenyl)-4 <i>H</i> -1-benzopyran-4-ones, <b>BP-n-I</b> .....	17
Figure 2.2	Synthetic scheme for the formation of 7-[[4-[4'-(( <i>S</i> )-2'-methylbutyloxy)carbonylphenyl]phenoxy}decyloxy]-3-(4'-substitutedphenyl)-4 <i>H</i> -1-benzopyran-4-ones, <b>BPI-R</b> .....	20
Figure 2.3	Synthetic scheme for the formation of 7-[[4-[(4-methoxyphenyl)diazenyl]phenoxy}alkyloxy]-3-(4'-methoxyphenyl)-4 <i>H</i> -1-benzopyran-4-ones, <b>AB-n-I</b> .....	22
Figure 2.4	Synthetic scheme for the formation of 1,3-bis{[3-(4'-decyloxyphenyl)-4 <i>H</i> -1-benzopyran-4-one-7-oxy]alkyloxy}benzenes, <b>BI-n-B</b> .....	25

Figure 3.1	FT-IR spectrum of 7-[{4-[4'-(( <i>S</i> )-2''-methylbutyloxy)carbonylphenyl]phenoxy}pentyloxy]-3-(4'-decyloxyphenyl)-4 <i>H</i> -1-benzopyran-4-one, <b>BP-5-I</b> .....	30
Figure 3.2	Structure of compound <b>BP-5-I</b> with complete atomic numbering .....	31
Figure 3.3	<sup>1</sup> H-NMR spectrum of 7-[{4-[4'-(( <i>S</i> )-2''-methylbutyloxy)carbonylphenyl]phenoxy}pentyloxy]-3-(4'-decyloxyphenyl)-4 <i>H</i> -1-benzopyran-4-one, <b>BP-5-I</b> .....	36
Figure 3.4	<sup>13</sup> C-NMR spectrum of 7-[{4-[4'-(( <i>S</i> )-2''-methylbutyloxy)carbonylphenyl]phenoxy}pentyloxy]-3-(4'-decyloxyphenyl)-4 <i>H</i> -1-benzopyran-4-one, <b>BP-5-I</b> .....	39
Figure 3.5	<sup>1</sup> H- <sup>1</sup> H COSY spectrum of 7-[{4-[4'-(( <i>S</i> )-2''-methylbutyloxy)carbonylphenyl]phenoxy}pentyloxy]-3-(4'-decyloxyphenyl)-4 <i>H</i> -1-benzopyran-4-one, <b>BP-5-I</b> .....	42
Figure 3.6	<sup>1</sup> H- <sup>13</sup> C HMQC spectrum of 7-[{4-[4'-(( <i>S</i> )-2''-methylbutyloxy)carbonylphenyl]phenoxy}pentyloxy]-3-(4'-decyloxyphenyl)-4 <i>H</i> -1-benzopyran-4-one, <b>BP-5-I</b> .....	43
Figure 3.7	<sup>1</sup> H- <sup>13</sup> C HMBC spectrum of 7-[{4-[4'-(( <i>S</i> )-2''-methylbutyloxy)carbonylphenyl]phenoxy}pentyloxy]-3-(4'-decyloxyphenyl)-4 <i>H</i> -1-benzopyran-4-one, <b>BP-5-I</b> .....	44
Figure 3.8	Optical photomicrographs for <b>BP-8-I</b> exhibiting (a) focal conic fan-shaped texture of SmA* phase and (b) same sample area showing SmC* phase with the development of a line pattern across the fans ....	48
Figure 3.9	(Left-right)-Formation of filaments during SmA*-N* phase transition observed for <b>BP-10-I</b> .....	48

Figure 3.10	Optical photomicrographs for <b>BP-10-I</b> showing (a) fan-shaped texture of N* phase and (b) dechiralization lines in the SmC* phase .....	48
Figure 3.11	A plot of transition temperatures, T against the number of methylene units, n in the spacer for <b>BP-n-I</b> .....	50
Figure 3.12	A DSC trace of <b>BP-10-I</b> during heating and cooling cycles at $\pm 5\text{ }^{\circ}\text{Cmin}^{-1}$ .....	51
Figure 3.13	The smectic layer spacing, <i>d</i> , for SmA* phase against the number of methylene units, n in the spacer for <b>BP-n-I</b> .....	53
Figure 3.14	Variation of smectic layer spacing, <i>d</i> against temperature for <b>BP-n-I</b> .	53
Figure 3.15	X-ray diffraction patterns for <b>BP-11-I</b> in (a) N* and (b) SmA* phases	55
Figure 3.16	FT-IR spectrum of 7-[{4-[4'-((S)-2"-methylbutyloxy)carbonylphenyl]phenoxy}decyloxy]-3-(4'-bromophenyl)-4 <i>H</i> -1-benzopyran-4-one, <b>BPI-Br</b> .....	57
Figure 3.17	A general molecular structure of <b>BPI-R</b> with complete atomic numbering .....	58
Figure 3.18	<sup>1</sup> H-NMR spectrum of 7-[{4-[4'-((S)-2"-methylbutyloxy)carbonylphenyl]phenoxy}decyloxy]-3-(4'-bromophenyl)-4 <i>H</i> -1-benzopyran-4-one, <b>BPI-Br</b> .....	61
Figure 3.19	<sup>13</sup> C-NMR spectrum of 7-[{4-[4'-((S)-2"-methylbutyloxy)carbonylphenyl]phenoxy}decyloxy]-3-(4'-bromophenyl)-4 <i>H</i> -1-benzopyran-4-one, <b>BPI-Br</b> .....	64
Figure 3.20	<sup>1</sup> H- <sup>1</sup> H COSY spectrum of 7-[{4-[4'-((S)-2"-methylbutyloxy)carbonylphenyl]phenoxy}decyloxy]-3-(4'-bromophenyl)-4 <i>H</i> -1-benzopyran-4-one, <b>BPI-Br</b> .....	67

Figure 3.21	$^1\text{H}$ - $^{13}\text{C}$ HMQC spectrum of 7-[{4-[4'-(( <i>S</i> )-2"-methylbutyloxy)carbonylphenyl]phenoxy}decyloxy]-3-(4'-bromophenyl)-4 <i>H</i> -1-benzopyran-4-one, <b>BPI-Br</b> .....	68
Figure 3.22	$^1\text{H}$ - $^{13}\text{C}$ HMBC spectrum of 7-[{4-[4'-(( <i>S</i> )-2"-methylbutyloxy)carbonylphenyl]phenoxy}decyloxy]-3-(4'-bromophenyl)-4 <i>H</i> -1-benzopyran-4-one, <b>BPI-Br</b> .....	69
Figure 3.23	A DSC trace of <b>BPI-Cl</b> during heating and cooling cycles at $\pm 5\text{ }^\circ\text{Cmin}^{-1}$ .....	72
Figure 3.24	Optical photomicrographs showing (a) oily streaks texture of $\text{N}^*$ phase for <b>BPI-CH<sub>3</sub></b> and (b) striated focal conic fans of $\text{SmA}^*$ -Cryst transition for <b>BPI-Br</b> .....	73
Figure 3.25	X-ray diffraction pattern of $\text{SmA}^*$ phase shown by <b>BPI-Br</b> .....	74
Figure 3.26	Dependence of substituents, R on transition temperatures, T.....	76
Figure 3.27	FT-IR spectrum of 7-[{4-[(4'-methoxyphenyl)diazenyl]phenoxy}pentyloxy]-3-(4'-methoxyphenyl)-4 <i>H</i> -1-benzopyran-4-one, <b>AB-5-I</b> .....	79
Figure 3.28	Structure of <b>AB-5-I</b> with complete atomic numbering.....	80
Figure 3.29	$^1\text{H}$ -NMR spectrum of 7-[{4-[(4'-methoxyphenyl)diazenyl]phenoxy}pentyloxy]-3-(4'-methoxyphenyl)-4 <i>H</i> -1-benzopyran-4-one, <b>AB-5-I</b> .....	82
Figure 3.30	$^{13}\text{C}$ -NMR spectrum of 7-[{4-[(4'-methoxyphenyl)diazenyl]phenoxy}pentyloxy]-3-(4'-methoxyphenyl)-4 <i>H</i> -1-benzopyran-4-one, <b>AB-5-I</b> .....	84

Figure 3.31	$^1\text{H}$ - $^1\text{H}$ COSY spectrum of 7-[[4-[(4'-methoxyphenyl)diazenyl]phenoxy}pentyloxy]-3-(4'-methoxyphenyl)-4 <i>H</i> -1-benzopyran-4-one, <b>AB-5-I</b> .....	87
Figure 3.32	$^1\text{H}$ - $^{13}\text{C}$ HMQC spectrum of 7-[[4-[(4'-methoxyphenyl)diazenyl]phenoxy}pentyloxy]-3-(4'-methoxyphenyl)-4 <i>H</i> -1-benzopyran-4-one, <b>AB-5-I</b> .....	88
Figure 3.33	$^1\text{H}$ - $^{13}\text{C}$ HMBC spectrum of 7-[[4-[(4'-methoxyphenyl)diazenyl]phenoxy}pentyloxy]-3-(4'-methoxyphenyl)-4 <i>H</i> -1-benzopyran-4-one, <b>AB-5-I</b> .....	89
Figure 3.34	A DSC trace of <b>AB-8-I</b> during heating and cooling cycles at $\pm 5\text{ }^\circ\text{Cmin}^{-1}$ .....	91
Figure 3.35	Optical photomicrographs for <b>AB-7-I</b> showing (a) N droplets and (b) N schlieren texture with twofold and fourfold brushes .....	92
Figure 3.36	A plot of transition temperatures, <i>T</i> against the number of methylene units, <i>n</i> in the spacer for <b>AB-<i>n</i>-I</b> .....	92
Figure 3.37	A plot of entropy change associated with the N-Iso transition, $\Delta S_{\text{NI}}/R$ against the number of methylene units, <i>n</i> in the spacer for <b>AB-<i>n</i>-I</b> .....	95
Figure 3.38	Molecular shapes of the all- <i>trans</i> conformation of (a) <b>AB-4-I</b> and (b) <b>AB-3-I</b> .....	95
Figure 3.39	FT-IR spectrum of 1,3-bis{[3-(4'-decyloxyphenyl)-4 <i>H</i> -1-benzopyran-4-one-7-oxy]butyloxy}benzene, <b>BI-4-B</b> .....	97
Figure 3.40	Structure of <b>BI-4-B</b> with complete atomic numbering .....	98
Figure 3.41	$^1\text{H}$ -NMR spectrum of 1,3-bis{[3-(4'-decyloxyphenyl)-4 <i>H</i> -1-benzopyran-4-one-7-oxy]butyloxy}benzene, <b>BI-4-B</b> .....	100

Figure 3.42	$^{13}\text{C}$ -NMR spectrum of 1,3-bis{[3-(4'-decyloxyphenyl)-4 <i>H</i> -1-benzopyran-4-one-7-oxy]butyloxy}benzene, <b>BI-4-B</b> .....	103
Figure 3.43	$^1\text{H}$ - $^1\text{H}$ COSY spectrum of 1,3-bis{[3-(4'-decyloxyphenyl)-4 <i>H</i> -1-benzopyran-4-one-7-oxy]butyloxy}benzene, <b>BI-4-B</b> .....	106
Figure 3.44	$^1\text{H}$ - $^{13}\text{C}$ HMQC spectrum of 1,3-bis{[3-(4'-decyloxyphenyl)-4 <i>H</i> -1-benzopyran-4-one-7-oxy]butyloxy}benzene, <b>BI-4-B</b> .....	107
Figure 3.45	$^1\text{H}$ - $^{13}\text{C}$ HMBC spectrum of 1,3-bis{[3-(4'-decyloxyphenyl)-4 <i>H</i> -1-benzopyran-4-one-7-oxy]butyloxy}benzene, <b>BI-4-B</b> .....	108
Figure 3.46	A DSC trace of <b>BI-5-B</b> during heating and cooling cycles at $\pm 5\text{ }^\circ\text{Cmin}^{-1}$ .....	110
Figure 3.47	A plot of transition temperatures, <i>T</i> against the number of methylene units, <i>n</i> in the spacer for <b>BI-n-B</b> .....	111
Figure 3.48	Optical photomicrographs showing (a) fan-shaped of SmA phase on left and broken fan-shaped of SmC phase on right for <b>BI-12-B</b> , (b) N phase for <b>BI-7-B</b> .....	112
Figure 3.49	Schlieren texture of (a) SmC <sub>anti</sub> and (b) SmC <sub>syn</sub> phases of <b>BI-10-B</b> . Two-brush defects with $s = \frac{1}{2}$ (marked with circle) are present only in anticlinic phase. Arrangement of molecules in synclinic and anticlinic smectic is shown schematically .....	112
Figure 3.50	Layer thickness against temperature in smectic phase for <b>BI-n-B</b> . In the inset the characteristic length corresponding to X-ray signals position in SmA phase (black squares) or nematic phase (open circles).....	114
Figure 3.51	Molecular conformations of <b>BI-3-B</b> : (a) most extended, $L_1$ (60.5 Å) and (b) strongly bent, $L_2$ (33.4 Å).....	116



Figure 3.52 Structures of smectic phases formed by (a) intercalated molecules in rod-shaped conformation and (b) molecules in bent-shaped conformation. Note that both structures show the same layer spacing 116

Figure 3.53 The low angle X-ray patterns for nematic phase (a) **BI-5-B** and (b) **BI-8-B**..... 117

Figure 3.54 A plot of clearing temperatures,  $T_c$  against the number of methylene units,  $n$  in the spacer for **BP-n-I**, **AB-n-I** and **BI-n-B** ..... 119

Figure C-1	DEPT 90 spectrum of 7-[{4-[4'-((S)-2"-methylbutyloxy)carbonylphenyl]phenoxy}pentyloxy]-3-(4'-decyloxyphenyl)-4 <i>H</i> -1-benzopyran-4-one, <b>BP-5-I</b> .....	137
Figure C-2	DEPT 135 spectrum of 7-[{4-[4'-((S)-2"-methylbutyloxy)carbonylphenyl]phenoxy}pentyloxy]-3-(4'-decyloxyphenyl)-4 <i>H</i> -1-benzopyran-4-one, <b>BP-5-I</b> .....	138
Figure C-3	DEPT 90 spectrum of 7-[{4-[4'-((S)-2"-methylbutyloxy)carbonylphenyl]phenoxy}decyloxy]-3-(4'-bromophenyl)-4 <i>H</i> -1-benzopyran-4-one, <b>BPI-Br</b> .....	139
Figure C-4	DEPT 135 spectrum of 7-[{4-[4'-((S)-2"-methylbutyloxy)carbonylphenyl]phenoxy}decyloxy]-3-(4'-bromophenyl)-4 <i>H</i> -1-benzopyran-4-one, <b>BPI-Br</b> .....	140
Figure C-5	DEPT 90 spectrum of 7-[{4-[(4'-methoxyphenyl)diazenyl]phenoxy}pentyloxy]-3-(4'-methoxyphenyl)-4 <i>H</i> -1-benzopyran-4-one, <b>AB-5-I</b> .....	141
Figure C-6	DEPT 135 spectrum of 7-[{4-[(4'-methoxyphenyl)diazenyl]phenoxy}pentyloxy]-3-(4'-methoxyphenyl)-4 <i>H</i> -1-benzopyran-4-one, <b>AB-5-I</b> .....	142
Figure C-7	DEPT 90 spectrum of 1,3-bis{[3-(4'-decyloxyphenyl)-4 <i>H</i> -1-benzopyran-4-one-7-oxy]butyloxy}benzene, <b>BI-4-B</b> .....	143
Figure C-8	DEPT 135 spectrum of 1,3-bis{[3-(4'-decyloxyphenyl)-4 <i>H</i> -1-benzopyran-4-one-7-oxy]butyloxy}benzene, <b>BI-4-B</b> .....	144

## LIST OF ABBREVIATION

%	Percent
$\Delta S_{NI}/R$	Entropy change of nematic-isotropic transition per gas constant
$^{\circ}\text{C}$	Degree Celsius
$^{\circ}\text{Cmin}^{-1}$	Degree Celsius per minute
$^{13}\text{C-NMR}$	Carbon nuclear magnetic resonance
$^1\text{H-NMR}$	Proton nuclear magnetic resonance
$\text{\AA}$	Angstrom
$\text{\AA K}^{-1}$	Angstrom per kelvin
$\text{BF}_3\cdot\text{EtO}_2$	Boron triflouride-diethyl ether complex
$\text{Br}_2\text{C}_n\text{H}_{2n}$	Dibromoalkane
$\text{CDCl}_3$	Deuterated chloroform
$\text{CH}_3\text{COCH}_3$	Acetone
COSY	Correlation spectroscopy
Cryst	Crystal phase
$d$	Layer spacing
d	Doublet
dd	Doublet of doublet
DEPT	Distortionless enhancement by polarization transfer
DMF	Dimethylformamide
DSC	Differential scanning calorimetry
FT-IR	Fourier transform infrared
FT-NMR	Fourier transform nuclear magnetic resonance
$\text{H}_2\text{SO}_4$ conc.	Concentrated sulfuric acid

HCl conc.	Concentrated hydrochloric acid
HMBC	Heteronuclear multiple bond correlation
HMQC	Heteronuclear multiple quantum correlation
Iso	Isotropic phase
<i>J</i>	Coupling constant
K <sub>2</sub> CO <sub>3</sub>	Potassium carbonate
KI	Potassium iodide
kJmol <sup>-1</sup>	Kilojoule per mole
KOH	Potassium hydroxide
<i>L</i>	Molecular length
<i>L</i> <sub>1</sub>	Molecular length of the most extended conformation
<i>L</i> <sub>2</sub>	Molecular length of the strongly bent conformers
LC	Liquid crystal
m	Multiplet
MeOH	Methanol
MeSO <sub>2</sub> Cl	Methansulfonyl chloride
MHz	Megahertz
N	Nematic phase
n	Number of methylene units
N*	Chiral nematic phase
NaNO <sub>2</sub>	Sodium nitrite
NaOH	Sodium hydroxide
POM	Polarising optical microscope
<i>P</i> <sub>s</sub> /nCcm <sup>-2</sup>	Spontaneous polarization in nanocoulomb per centimeter squared unit

s	Singlet
SmA	Smectic A phase
SmA*	Chiral Smectic A phase
SmA <sub>c</sub>	Intercalated smectic A phase
SmC	Smectic C phase
SmC*	Chiral smectic C phase
SmC <sub>anti</sub>	Anticlinic smectic C phase
SmC <sub>syn</sub>	Synclonic smectic C phase
t	Triplet
T <sub>c</sub>	Clearing temperature
TGB	Twist grain boundary
T <sub>m</sub>	Melting temperature
TMS	Tetrametylsilane
T <sub>NI</sub>	Nematic-isotropic transition temperature
v/v	Volume per volume
XRD	X-ray Diffraction
δ/ppm	Chemical shift in part per million unit
θ	Tilt angle
ν/cm <sup>-1</sup>	Wavenumber in centimeter unit
z	Layer normal

# SINTESIS, PENCIRIAN DAN SIFAT MESOMORFIK BAGI OLIGOMER ISOFLAVON SIMETRI DAN BUKAN SIMETRI

## ABSTRAK

Empat siri baru oligomer hablur cecair simetri dan bukan simetri yang berdasarkan isoflavon telah disintesis dan dicirikan. Oligomer ini terdiri daripada tiga siri dimer bukan simetri, iaitu 7-[[4-[4'-((S)-2''-metilbutiloksi)karonilfenil]fenoksi]alkiloksi]-3-(4'-desiloksifenil)-4*H*-1-benzopiran-4-on (**BP-n-I**), 7-[[4-[4'-((S)-2''-metilbutiloksi)karonilfenil]fenoksi]desiloksi]-3-(4'-tertutukargantifenil)-4*H*-1-benzopiran-4-on (**BPI-R**) dan 7-[[4-[4'-metoksifenil]diazetil]fenoksi]alkiloksi]-3-(4'-metoksifenil)-4*H*-1-benzopiran-4-on (**AB-n-I**), dan satu siri trimer simetri: 1,3-bis[[3-(4'-desiloksifenil)-4*H*-1-benzopiran-4-on-7-oksi]alkiloksi]benzena (**BI-n-B**). Kesemua oligomer mesogenik tersebut berbeza antara satu sama lain daripada segi kumpulan mesogen dan panjang spaser. Struktur molekul bagi sebatian oligomer ini telah diterangkan melalui spektroskopi CHN, FT-IR, <sup>1</sup>H-NMR, <sup>13</sup>C-NMR, <sup>1</sup>H-<sup>1</sup>H COSY, <sup>1</sup>H-<sup>13</sup>C HMQC dan <sup>1</sup>H-<sup>13</sup>C HMBC sebelum penyiasatan sifat hablur cecair dijalankan dengan menggunakan POM, DSC and XRD. Mono- dan/atau polimorfisma telah diperhatikan bagi kesemua oligomer tersebut. Oligomer ini mempamerkan pelbagai fasa termasuk fasa nematik kiral (N\*), fasa smektik A selapis dan 'intercalated' (SmA dan SmA<sub>c</sub> masing-masing), fasa smektik C 'synclinic' (SmC<sub>syn</sub>) dan 'anticlinic' (SmC<sub>anti</sub>) mono- dan enantiotropik. Tambahan pula, kesan ganjil-genap yang ketara dalam suhu peralihan fasa (T<sub>m</sub> dan T<sub>c</sub>) telah diperhatikan bagi **BP-n-I**, **AB-n-I** dan homolog pendek **BI-n-B** (n = 3-7) apabila panjang spaser berubah. Suatu ciri khas yang perlu dikemukakan ialah tingkah laku jenis *de Vries* yang dipamerkan oleh homolog terpendek bagi **BP-n-I**. Selain itu, suatu perubahan geometri daripada bentuk rod 'intercalated' bagi

homolog pendek kepada bentuk bengkok bagi homolog panjang dalam **BI-n-B** menyebabkan pemerhatian tingkah laku mesomorfik yang luar biasa yang mana trimer pendek dan panjang mempamerkan SmA dan/atau fasa metastabil SmC manakala homolog dengan panjang spaser perantaraan bersifat nematogenik dengan julat suhu yang luas.

# SYNTHESIS, CHARACTERIZATION AND MESOMORPHIC PROPERTIES OF SYMMETRIC AND NON-SYMMETRIC ISOFLAVONE OLIGOMERS

## ABSTRACT

Four new series of symmetric and non-symmetric isoflavone-based liquid crystal oligomers have been synthesized and characterized. These oligomers comprised of three series of non-symmetric dimers, namely 7-[{4-[4'-((*S*)-2''-methylbutyloxy)carbonylphenyl]phenoxy}alkyloxy]-3-(4'-decyloxyphenyl)-4*H*-1-benzopyran-4-ones (**BP-n-I**), 7-[{4-[4'-((*S*)-2''-methylbutyloxy)carbonylphenyl]phenoxy}decyloxy]-3-(4'-substitutedphenyl)-4*H*-1-benzopyran-4-ones (**BPI-R**) and 7-[{4-[(4'-methoxyphenyl)diazenyl]phenoxy}alkyloxy]-3-(4'-methoxyphenyl)-4*H*-1-benzopyran-4-ones (**AB-n-I**), and a series of symmetric trimers: 1,3-bis[{3-(4'-decyloxyphenyl)-4*H*-1-benzopyran-4-one-7-oxy}alkyloxy]benzenes (**BI-n-B**). All oligomeric mesogens differ from one another in term of mesogenic moieties and spacer length. The molecular structures of these oligomers were elucidated via CHN, FT-IR, <sup>1</sup>H-NMR, <sup>13</sup>C-NMR, <sup>1</sup>H-<sup>1</sup>H COSY, <sup>1</sup>H-<sup>13</sup>C HMQC and <sup>1</sup>H-<sup>13</sup>C HMBC spectroscopy prior to the investigation of their liquid crystalline properties using POM, DSC and XRD. Mono- and/or polymorphism were observed in all oligomers. They exhibited a rich variety of phases including mono- and enantiotropic chiral nematic (N\*), monolayer and intercalated smectic A (SmA and SmA<sub>c</sub>, respectively), synclinic (SmC<sub>syn</sub>) and anticlinic smectic C (SmC<sub>anti</sub>) phases. Furthermore, pronounced odd-even effect in phase transition temperatures (T<sub>m</sub> and T<sub>c</sub>) upon varying the spacer length was observed for **BP-n-I**, **AB-n-I** and short homologues of **BI-n-B** (n = 3-7). One special feature worth mentioning was the de Vries type behaviour exhibited by the shortest homologue of **BP-n-I**. Apart from this, a crossover of



geometry from intercalated rod-shaped for short homologues to bent-shaped for long homologues in **BI-n-B** had resulted in the observation of an unusual mesomorphic behaviour wherein short and long trimers exhibited SmA and/or metastable SmC phase(s) while homologues with intermediate spacer length were purely nematogenic with broad temperature range.

## 1.0 INTRODUCTION

### 1.1 Liquid crystals

Liquid crystals (LCs) were first discovered by Fridrich Reinitzer, an Austrian Botanist in 1888. Reinitzer observed a strange behaviour of a material known as cholesteryl benzoate extracted from carrots (Reinitzer, 1888). This material has two distinct melting points. At 145.5 °C, it melted into a cloudy fluid prior to turning into a clear solution at 178.5 °C. Later, Reinitzer had discovered and described three important features of cholesteric liquid crystals (this name was coined by Georges Friedel in 1922): the existence of two melting points, the reflection of circularly polarized light and the ability to rotate the polarization direction of light. Further investigations of those phenomena were then carried out by Otto Lehmann, a German physicist (Collings and Hird, 1997).

Liquid crystal is a state of matter that is intermediate between a solid crystalline and an isotropic liquid. Unlike a solid crystal in which molecules are positioned in fixed orientations with no translational freedom, liquid crystals possess some orientational order and little or no positional order. Similar to molecules in a liquid phase, liquid crystals molecules are able to move freely but remain oriented to a common axis, called a director. The arrangement of molecules in each phase is shown in Figure 1.1.

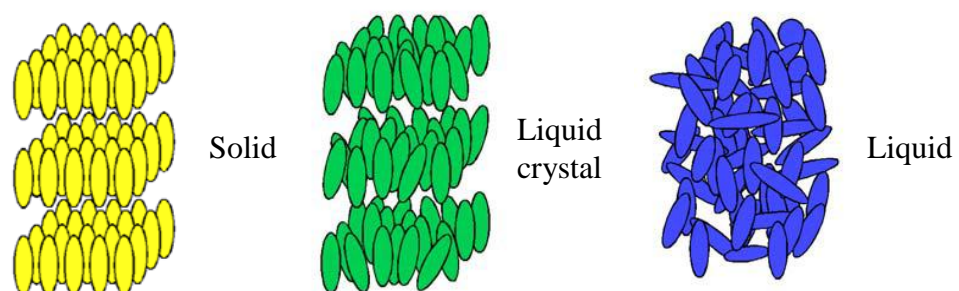


Figure 1.1: Arrangement of molecules in solid, liquid crystal and liquid (Shakhashiri, 2007).

## **1.2 Types of liquid crystals**

LCs can be divided into two classical categories: (i) lyotropic LCs (amphiphilic mesogens) which consist of two or more components that exhibit liquid crystalline properties in certain concentration range; (ii) thermotropic LCs (non-amphiphilic anisometric mesogens) which exhibit a variety of phases as temperature is changed. However, thermotropic LCs remain the focus of this study and hence, lyotropic LCs will not be discussed further.

## **1.3 Mesophases**

Typically, nematic and smectic are the two major types of mesophases, although many mesophases have been discovered in hitherto reported literatures (for the past 120 years). Among the many reported mesophases are the soft crystal phase, frustrated twist grain boundary (TGB) phases, chiral tilted smectic phases (exhibited by ferroelectric liquid crystals that include the chiral smectic C (SmC\*) subphases) and the banana phases.

### **1.3.1 Nematic phase**

Molecules in the nematic (N) phase have orientational order but no positional order. On average, these molecules are all aligned towards a similar direction, referred to as the director (Figure 1.2 (a)) (Singh, 2000).

#### **1.3.1.1 Cholesteric phase**

The cholesteric phase is also known as a chiral nematic (N\*) phase in which the N phase is composed or induced by chiral molecules. In the N\* phase as shown in Figure 1.2 (b), the molecular orientation in a plane rotates spirally in a direction perpendicular to the plane. The preferred orientation of molecules in N\* forms a

helical structure with the helical axis perpendicular to the director (Devi and Bhattacharjee, 2010).

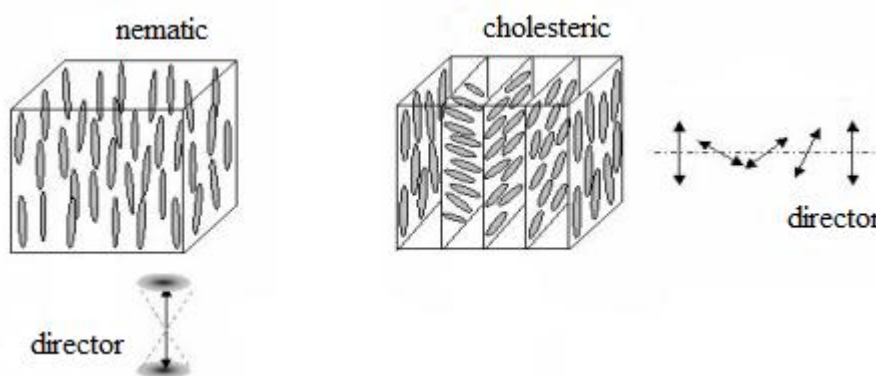


Figure 1.2: Diagrammatic representation of (a) N and (b) N\* phases (Devi and Bhattacharjee, 2010).

### 1.3.2 Smectic phase

#### 1.3.2.1 Smectic A phase

Molecules in smectic phases are ordered in layers and the translation of molecules from one layer to another is limited. Within these layered systems, a variety of molecular arrangements is possible. In the simplest, least ordered orthogonal smectic A (SmA) phase, there is no positional order within each layer and the long axes of the molecules are on average, positioned perpendicular to the layers (Figure 1.3 (a)) (Demus and Richter, 1980).

#### 1.3.2.2 Smectic C phase

The smectic C (SmC) phase differs from SmA phase in term of molecular arrangement in which the molecules in the SmC phase are uniformly tilted at an angle,  $\theta$ , relative to the layer normal,  $z$  (Figure 1.3 (b)). In general, the tilt angle increases with decreasing temperature.

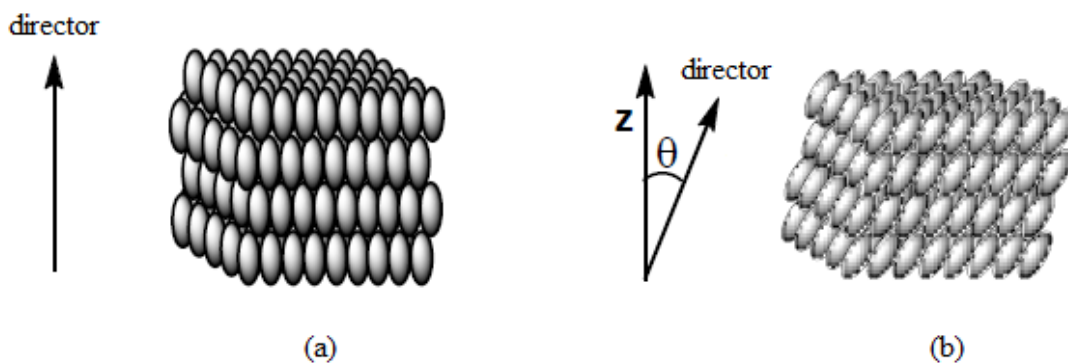


Figure 1.3: Molecular arrangement in (a) SmA and (b) SmC phases ("Lemieux Group Organic Materials," 2006).

### 1.3.2.3 Chiral smectic phase

In a chiral smectic phase, for example, the chiral smectic C ( $\text{SmC}^*$ ) phase, the molecules have positional ordering in a layered structure (as in other smectic phases), with the molecules tilted by a finite angle with respect to the layer normal. In  $\text{SmC}^*$  phase, a bulk electrical polarization referred to as the spontaneous polarization ( $P_s$ ), is present in the absence of any electrical field. These materials are (in general) ferroelectric. However, in the absence of external constraints, the  $\text{SmC}^*$  phase forms a macroscopic helical structure in which the  $P_s$  of vector rotates from one layer to another relative to the helical axis and averages out to zero over a full helical pitch (Figure 1.4) (Collings and Hird, 1997). In this phase, the orientation of the tilt can be influenced by an electric field, and therefore, it can be used in displays, that in theory can be switched much faster than conventional nematic displays.

## 1.4 Liquid crystal oligomers

Research activity in LC oligomers can be traced back to the early 1980s, especially the development of semi-flexible main chain LC polymers (Ober *et al.*, 1984). These oligomers consisted of mesogenic units connected by flexible spacers. LC oligomers attracted considerable amount of attention as these compounds are

referred to as models for the semi-flexible main chain liquid crystal polymers (Imrie and Henderson, 2002; Pal *et al.*, 2007). The remaining sections of this chapter will focus on the mesomorphic behaviours of LC dimers and trimers which are the scope of this study.

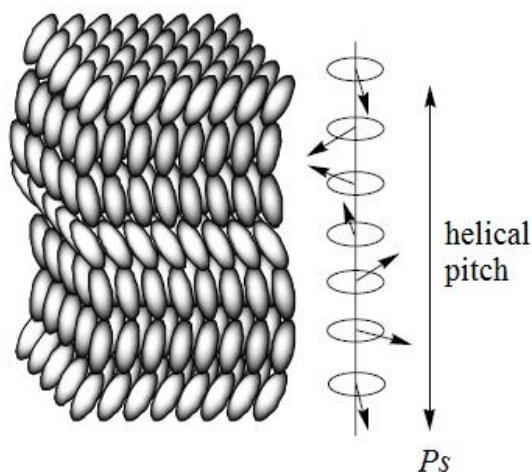


Figure 1.4: A SmC\* material showing the rotation of tilted director from layer to layer forming a helical structure (Clark and Lagerwall, 1980).

#### 1.4.1 Liquid crystal dimers

LC dimers are the shortest liquid crystal oligomers. They composed of molecules containing two conventional mesogenic units connected by a flexible spacer, most commonly an alkyl chain. A symmetric dimer possesses two identical mesogenic moieties connected by a flexible spacer, while a non-symmetric dimer is formed by two different mesogenic units linked through a flexible spacer.

#### 1.4.2 Liquid crystal trimers

A trimeric liquid crystal contains three mesogenic cores joined by two flexible spacers. In a similar manner to liquid crystal dimers, LC trimers can also be classified as symmetric and non-symmetric. For LC trimers, asymmetry can be introduced to their molecular structures by incorporating different mesogenic units

(either two or all three are different), flexible spacer or terminal chain length, terminal groups or some combination of these structural features.

## **1.5 Structure-property relationship of liquid crystal oligomers**

### **1.5.1 Phase behaviour in liquid crystal oligomers**

A unique characteristic which has been noted for symmetric LC dimers is the decreasing tendency to exhibit smectogenic properties upon increasing spacer length (Date *et al.*, 1992). For many dimeric LC, the smectic phase behaviour was also found to be suppressed when their mesogenic moieties (monomers) are smectogenic (Griffin and Britt, 1981). This phenomenon has been attributed to an increase in the overall molecular flexibility. It may be argued that the two rigid cores are joined by a flexible segment, but nevertheless the "center" of the structure is flexible.

Furthermore, it is known that dimers with long terminal tails are able to promote smectic behaviour regardless of the spacer length (Luckhurst and Gray, 1979). Some of them even exhibited a rich polymorphism of smectic phases, for example,  $\alpha,\omega$ -bis(4-(4'-n-decyloxyphenylethynyl)phenoxy)alkanes, which were reported by Rozhanskii I. L. (Rozhanskii *et al.*, 1996). A simple relationship between the occurrence of smectic behaviour and the molecular structure of symmetric dimers was also deduced from the studies on  $\alpha,\omega$ -bis(4-*n*-alkyl-anilinebenzylidene-4'-oxy)alkanes (Date *et al.*, 1992). In order to obtain smectic properties, the terminal chain length must be greater than half the spacer length. Otherwise, N behaviour was observed. Generally, a simple monolayer smectic phase was observed for symmetric LC dimers containing long terminal chain which is thought to be stabilized by microphase segregation of three weakly distinct parts: terminal chain, mesogenic moiety and flexible spacer (Figure 1.5 (a)) (Imrie and Henderson, 2002).

Similar to LC dimers, increasing the spacer length does not necessary promote smectic behaviour in LC trimer. However, it was found that two homologues of a reported series of nematogenic symmetric LC trimers, 4,4'-bis[ $\omega$ -((4-cyanobiphenyl-4'-yloxy)alkoxy)alkoxy]biphenyls exhibited an additional monotropic SmA phase (Imrie and Luckhurst, 1998), whilst the corresponding dimeric series,  $\alpha,\omega$ -bis(4,4'-cyanobiphenyloxy)alkanes were exclusively nematogens (Emsley *et al.*, 1984). Thus, smectic phase formation was more favourable for LC trimers than dimers with respect to these series. It was suggested that the enhanced smectic behaviour of this trimeric series may be attributed to a favourable specific interaction between the electron-rich biphenyl and the high electron affinity of the cyanobiphenyl moieties (Imrie *et al.*, 2009).

### 1.5.2 Layer arrangement of smectic phase in liquid crystal oligomers

In general, symmetric dimers exhibit monolayer smectic phase, while non-symmetric dimers tend to arrange in intercalated (Figure 1.5 (b)) or interdigitated (Figure 1.5 (c)) smectic organizations (Attard *et al.*, 1994; Blatch and Luckhurst, 2000). One of such examples is the  $\alpha$ -(4-cyanobiphenyl-4'-yloxy)- $\omega$ -[4-(5-alkylpyrimidine-2-yl)phenyl-4''-oxy]alkanes (Yoshizawa *et al.*, 2006). In the intercalated smectic phase, the smectic layer periodicity,  $d$  is approximately half the molecular length,  $L$  ( $d/L \approx 0.5$ ). The intercalated arrangement is resulted from a specific interaction between the unlike mesogenic units enhanced by an entropy gain resulting from the homogeneously mixing of such groups (Blatch *et al.*, 1997). The electrostatic quadrupolar interaction between the different mesogens having quadrupole moments of opposite signs is also believed to be another possible stabilizing factor (Blatch *et al.*, 1995). In some cases, however, symmetric dimers are also known to exhibit intercalated mesophases (Watanabe *et al.*, 1993). Contrary to



intercalated smectic phase, the layer thickness in interdigitated smectic phase is more than the length of one molecule but less than the length of two molecules,  $L < d < 2L$ . The driving force for this phase is however, not confined to only the presence of two unlike cores in the structure, as electrostatic interactions between certain groups like the polar and polarisable cyanobiphenyl groups in 1-(Cholest-5-en-3 $\beta$ -oxy)- $\omega$ -(4-cyanobiphenyl-4'-oxy)alkanes, is known to play a key role in inducing interdigitation (Marcelis *et al.*, 2003).

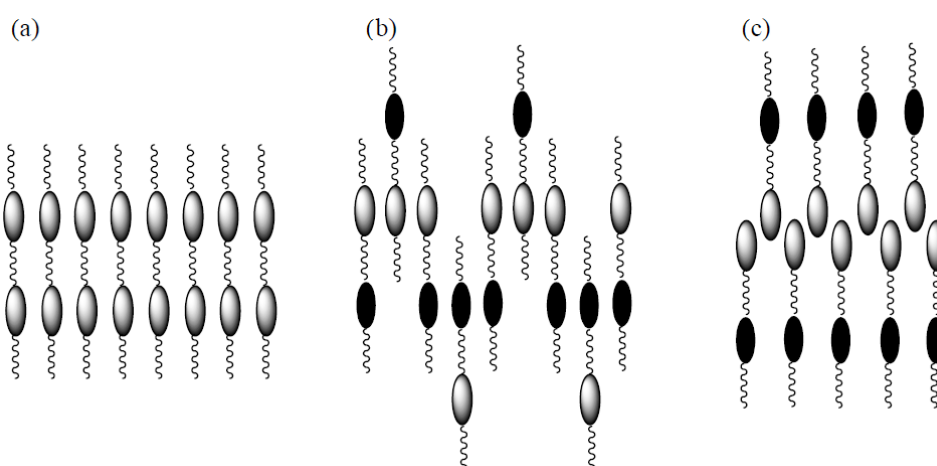


Figure 1.5: Diagrammatic representation of SmA arrangements in dimeric liquid crystals, (a) monolayer, (b) intercalated and (c) interdigitated (Imrie and Henderson, 2002).

Similar to LC dimers, most of the reported symmetric LC trimers have conventional monolayer smectic phase (Centore *et al.*, 1990; Yoshizawa *et al.*, 2007). Interestingly, a triply intercalated smectic phase ( $d/L \approx 0.3$ ) was found for several reported non-symmetric trimers (Donaldson *et al.*, 2011; Henderson and Imrie, 2005; Marcelis *et al.*, 2007). The driving force for the formation of this phase is considered to be electrostatic interactions between electron rich and electron deficient segments of the molecules.

### 1.5.3 Odd-even effect in liquid crystal oligomers

Strong odd-even effects are usually observed for dimeric liquid crystals due to the parity of the spacer (Watanabe *et al.*, 1993). The odd-even effect can be understood as a result of a conformational constraint whereby the molecules with an odd-parity spacer tend to assume a bent conformation with the two mesogens tilted and inclined to each other (Figure 1.6 (a)). In the even-parity spacer compounds, the mesogenic groups are more likely to have a *zigzag* conformation in which the mesogenic units are anti-parallel to each other (Figures 1.6 (b)) (Imrie and Henderson, 2007; Watanabe *et al.*, 2000). That is why LC dimers with odd-parity spacers have a stronger tendency to form SmC-like phases while even-parity homologues and analogues form SmA phases (Niori *et al.*, 1995; Watanabe *et al.*, 1993). In 1999, some additional striking properties of dimers with a flexible alkylene spacer were discovered (Choi *et al.*, 1999; Watanabe *et al.*, 1998). Some LC dimers with odd number of flexible units between the two mesogenic moieties adopted a bent conformation resulting in a liquid crystalline phase with electro-optical switching properties. Watanabe J. reported a chiral, anticlinic and antiferroelectric smectic phase formed by an achiral twin dimer with two identical mesogenic groups connected by an odd-parity spacer (Watanabe *et al.*, 1998). Surprisingly, switching behaviour was also observed in dimers with an even number of flexible units in the central spacer (Prasad, 2001; Prasad *et al.*, 2000,2001). However, no reasonable rationale for this observation was given.



Figure 1.6: Diagrammatic representation of dimeric molecules with (a) an odd and (b) an even number of flexible units between two mesogenic moieties.

The odd-even effect in transition temperatures and associated entropy changes observed for LC dimers are also found in trimeric liquid crystals as the length and parity of the spacers are varied, in which the even members exhibit higher values (Henderson *et al.*, 2004; Imrie and Luckhurst, 1998). The magnitude of the alternation exhibited by the transition temperatures and associated entropy changes of the trimers are considerably greater than that exhibited by their analogous dimers on a relative scale (Imrie and Henderson, 2002). This trend is to be expected given the increase in shape anisotropy on passing from dimeric to trimeric molecules (Imrie *et al.*, 2009). If a trimer is considered in its most extended all-*trans* conformation, two distinct molecular shapes are obtained depending on the parity of the spacers. The two outer mesogenic units of odd-parity trimers are inclined with respect to the central unit giving them a stretched ‘S’ shape (Figure 1.7 (a)), whereas in an even-parity trimer, all the three mesogenic units are co-parallel, resulting in an extended rod-like molecular structure (Figure 1.7 (b)). The even-parity trimers, therefore, have an enhanced shape anisotropy which allows the molecules to pack more efficiently in the liquid crystal phase, thus giving higher transition temperatures and entropy changes (Imrie and Henderson, 2007).

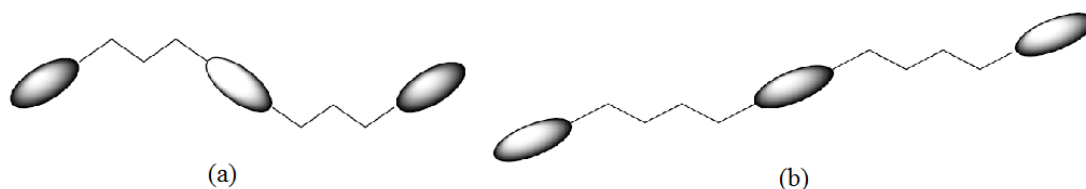


Figure 1.7: Molecular shapes of the all-*trans* conformation of trimers containing (a) odd- and (b) even-parity flexible spacers.

#### 1.5.4 Chirality effect on liquid crystalline properties of oligomers

Chirality in liquid crystalline systems has been a major area of considerable research interest for both technological and fundamental reasons (Goodby, 1991; Mallia and Tamaoki, 2004). The presence of chiral centres in a mesogen can tremendously modify the organisation of the mesophases. Novel structures like the helical superstructure of N\* and SmC\* phases were induced (Nishiyama *et al.*, 2001,2002a). Tilted chiral smectic phases could exhibit spontaneous polarization and thus these mesophases were pyroelectric (Dierking, 2003). Coupling between chirality and oligomeric structures could also produce novel phenomena. Blatch and co-workers reported that chirality exhibited a dependence on the parity of the spacer, whereas blue phase I behaviour was observed in a very narrow temperature range (0.6 K) between isotropic liquid (Iso) and N\* phases for the odd, non-symmetric dimers, whereas a direct Iso–N\* transition was observed for the even, non-symmetric dimers (Blatch *et al.*, 1997). Nishiyama I. also described unusual chirality-dependent phase behaviour of their designed chiral dimers, which showed ferroelectric and antiferroelectric phases with high values of tilt angles (Nishiyama *et al.*, 2001,2002b). A direct ferroelectric smectic-to-isotropic phase transition was observed along with an isotropic to isotropic transition in the liquid phase; the racemic analogue, however, exhibited N-SmC phase sequence. Furthermore, Yelamaggad C. V. reported the mesomorphic properties of chiral unsymmetrical LC trimers: cholesteryl 6-{4-[4-[(4-butylphenylazophenoxy)butoxy]phenylethynyl]phenoxy} hexanoate, with three non-identical mesogenic units exhibiting both the twist grain boundary (TGB) and undulating TGB (UTGB) phases depending on the parity of the spacers (Yelamaggad *et al.*, 2000; Yelamaggad *et al.*, 2001).

## 1.6 Liquid crystals oligomers incorporating isoflavone moiety

The effort in modifying the existing molecules, particularly natural products has well been considered as a viable approach that can lead to some novel and new compounds showing liquid crystalline properties (Hirose *et al.*, 1989). Isoflavone made up the largest group of natural isoflavonoids (Adlercreutz *et al.*, 1986). The pharmaceutical properties of isoflavones have been well documented (Boland and Donnelly, 1998; Chen *et al.*, 2008; Kohen *et al.*, 2007). Similar to many natural products possessing heterocycles in their structures including flavone and coumarin derivatives, isoflavone-based compounds in biological systems show remarkable liquid crystalline properties (Hirose *et al.*, 1989). Figure 1.8 depicts a general structure of isoflavone. Chudgar N. K. and co-workers were the first researchers who synthesized and characterized liquid crystals derived from isoflavone (Chudgar *et al.*, 1991). Over the years, the mesogenicity of several isoflavone derivatives with classical calamitic structures containing one or two terminal chains have also been documented (Belmar, 1999; Chudgar *et al.*, 1995; Chudgar and Shah, 1991). In order to study and understand the effect of different structural changes on the mesomorphism of these compounds, various modifications on existing molecules have been made, keeping in view the molecular geometry of the isoflavone moiety. The influence of different functional linkages, terminal chain length and polar terminal groups on the mesogenicity of liquid crystalline compounds have been reported (Yeap *et al.*, 2009b; Yeap *et al.*, 2008a; Yeap *et al.*, 2007; Yeap *et al.*, 2008b). However, liquid crystal oligomers incorporating isoflavone moiety have not been reported. In order to establish the structure-property relationship of the isoflavone-based oligomers, four series of oligomeric liquid crystalline compounds with various structural modifications have been prepared.

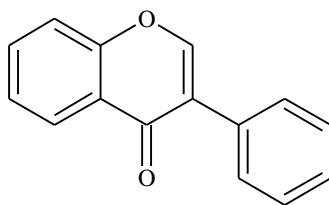


Figure 1.8: A general structure of isoflavone (3-phenyl-4*H*-1-benzopyran-4-one).

## 1.7 Research objectives

The objectives of this study are:

- a) To synthesize and characterize new symmetric and non-symmetric isoflavone-based, thermotropic liquid crystal oligomers.
- b) To investigate the effect of chirality on the liquid crystalline properties of these oligomers.
- c) To investigate the structure-property relationship of these oligomers.

## 2.0 EXPERIMENTAL

### 2.1 Chemicals

From Acros Organic, Belgium: 1,4-dibromobutane, 99%; 1,5-dibromopentane, 97%; 1,6-dibromohexane, 98%; 1,8-dibromooctane, 98%; 1,9-dibromononane, 97%; 1,10-dibromodecane, 97%; 1,11-dibromoundecane, 98%; 1,12-dibromododecane, 96%; 4-hydroxyphenylacetic acid, 98%; 4-methylphenylacetic acid, 99% and 4-methoxyphenylacetic acid, 99%. From Tokyo Chemical Industry, Japan: 4-bromophenylacetic acid, 98%; 4-chlorophenylacetic acid, 97%; 4-fluorophenylacetic acid, 98% and 4-(4-hydroxyphenyl)benzoic acid, 98%. From Sigma-Aldrich, United States of America: resorcinol, 99%; 1-bromodecane, 98%; phenol, 99%; 4-methoxyaniline, 99% and 1,7-dibromoheptane, 97%. From Fisher Scientific, United Kingdom: potassium carbonate anhydrous, 99%; potassium iodide, 99% and hydrochloric acid, 37%. From R & M Chemical, United Kingdom: sodium nitrite, 98%; sodium hydroxide, 99%; potassium hydroxide, 85%. From Fluka, Switzerland: 1,3-dibromopropane and 99%; (*S*)-(-)-2-methyl-1-butanol, 95%. From Merck, Germany: boron trifluoride-diethyl ether complex, 50%; methanesulfonyl chloride, 99% and phenylacetic acid, 99%. From Avantor, United States of America: sulfuric acid, 98%. All chemicals were used without further purification.

### 2.2 Instruments

- CHN microanalyses were carried out on a Perkin Elmer 2400 LS Series CHNS/O analyzer at the School of Chemical Sciences, Universiti Sains Malaysia (USM).

- Fourier Transform Infrared (FT-IR) data were recorded using a Perkin Elmer 2000-FTIR spectrophotometer at the School of Chemical Sciences, USM.
- 1D and 2D Fourier Transform Nuclear Magnetic Resonance (FT-NMR) were performed using a Bruker-Avance 300MHz, 400MHz or 500MHz ultrashield spectrometer at the School of Chemical Sciences, USM.
- Phase transition temperatures and enthalpy values of the synthetic compounds were measured using the following instruments:
  - i. Seiko DSC6200R differential scanning calorimetry (DSC) at Tokyo Institute of Technology University, Japan.
  - ii. TA Instrument DSC2000 at the Chemistry Department, Warsaw University.
  - iii. Mettler Toledo DSC822<sup>e</sup> equipped with a TSO 801RO sample robot at the School of Natural and Computing Sciences, University of Aberdeen.
- Textures of the mesophases were studied using a Carl Zeiss polarizing microscope equipped with a Linkam LTS350 hot stage and TMS94 temperature controller at the Liquid Crystal Research Laboratory, School of Chemical Sciences, USM.
- Layer spacing of liquid crystalline compounds during mesophase transitions was measured over a range of temperatures using a Bruker D8 Discover and GADDS system at the Laboratory of Dielectrics and Mechanics of the Chemistry Department, University of Warsaw.



- Dechiralization line distance that corresponds to the helical pitch was measured by using the pictures obtained from Zeiss microscope Axio Imager at the Chemistry Department, University of Warsaw.

## 2.3 Synthesis

All compounds were synthesized and purified at normal atmospheric pressure by conventional method unless stated otherwise.

### 2.3.1 Preparation of 7-[[4-[4'-((*S*)-2''-methylbutyloxy)carbonylphenyl]phenoxy}alkyloxy]-3-(4'-decyloxyphenyl)-4*H*-1-benzopyran-4-ones, BP-*n*-I (*n* = 3-12)

The aforementioned were synthesized according to the synthetic routes shown in Figure 2.1.

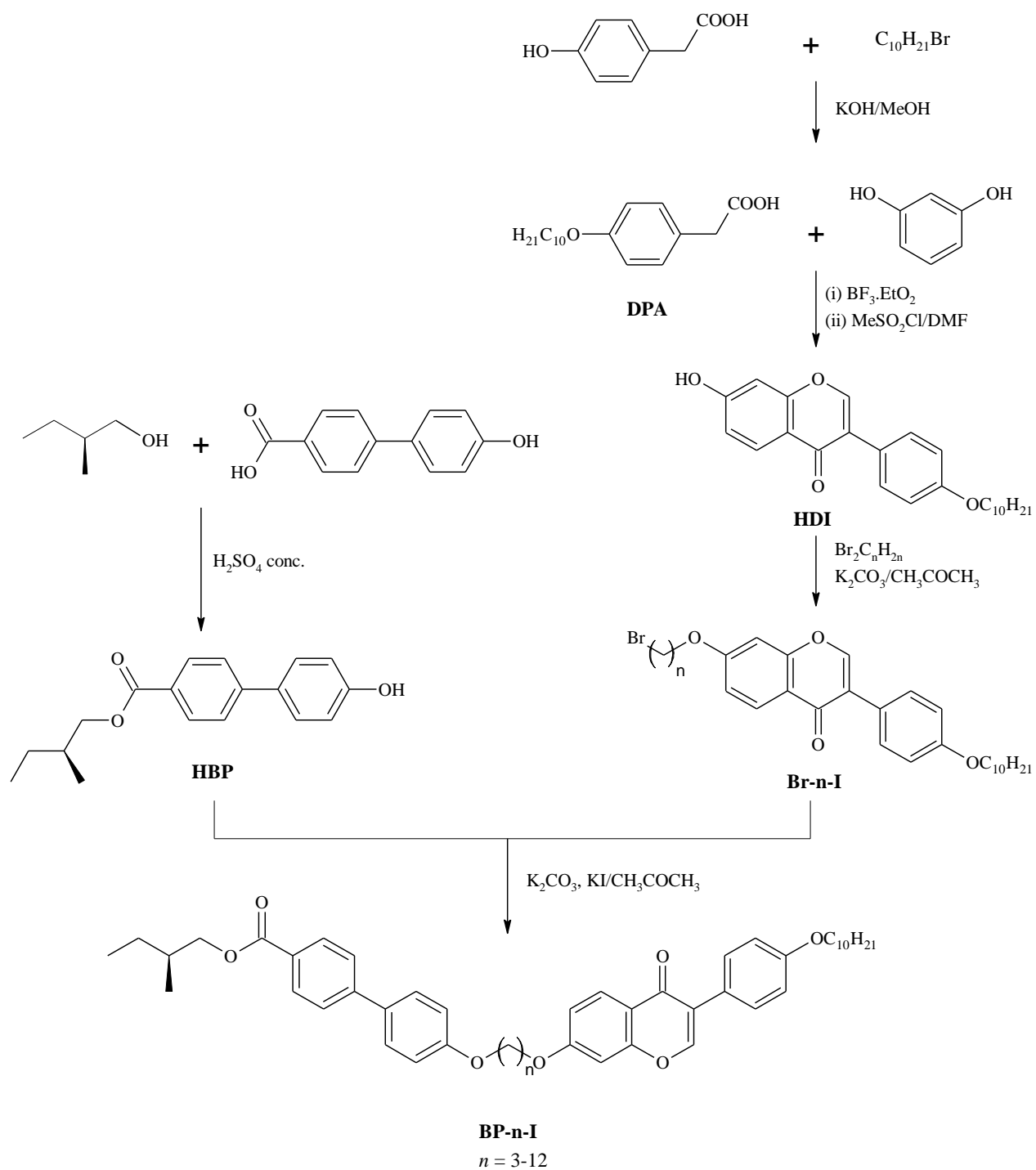


Figure 2.1: Synthetic scheme for the formation of 7-[[4-[4'-((S)-2''-methylbutyloxy)carbonylphenyl]phenoxy}alkyloxy]-3-(4'-decyloxyphenyl)-4*H*-1-benzopyran-4-ones, **BP-n-I**.

#### **2.3.1.1 Synthesis of (S)-(-)-2-methylbutyl-4'-(4''-hydroxyphenyl)benzoate, HBP**

4-(4-hydroxyphenyl)benzoic acid (2.15 g, 0.01 mol) was added to (S)-(-)-2-methyl-1-butanol (30 mL), which served as a reactant and solvent. A catalytic amount of concentrated H<sub>2</sub>SO<sub>4</sub> was added dropwise and the reaction mixture heated to 90 °C for 24 hours. The resulting solution was cooled to room temperature and excess solvent was removed via evaporation. The crude product was then recrystallized from a solution of hexane and chloroform (1:2, v/v).

#### **2.3.1.2 Synthesis of 4-decyloxyphenylacetic acid, DPA**

2 equiv. of potassium hydroxide in methanol was added to a cold methanolic solution containing 4-hydroxyphenylacetic acid (10.70 g, 0.07 mol). Subsequently, 1.2 equiv. of 1-bromodecane was added and the reaction mixture was heated under reflux for 18 hours. The solvent was subsequently removed and the reaction mixture was neutralized with 10 % of aqueous hydrochloric acid. The crude product was filtered off, washed thoroughly with water and recrystallized from methanol.

#### **2.3.1.3 Synthesis of 7-hydroxy-3-(4'-decyloxyphenyl)-4*H*-1-benzopyran-4-one, HDI**

**HDI** was synthesized according to the modified method reported by Wahala K. (Wahala and Hase, 1991). Under nitrogen atmosphere, a mixture containing 4-decyloxyphenylacetic acid (8.50 g, 0.03 mol) and 1.1 equiv. of resorcinol in BF<sub>3</sub>.Et<sub>2</sub>O was heated for 4 hours at 70-75 °C. The reaction mixture was then cooled down to room temperature and dry DMF was added. The mixture was again heated to 50 °C and a solution of 3 equiv. of methanesulfonyl chloride in dry DMF was added slowly. After heating the reaction mixture for 1.5 hours at 75-80 °C, it was

poured into a rapid stirring of ice water bath upon which the crude product was formed. The product was then recrystallized from methanol.

#### **2.3.1.4 Syntheses of 7-(n-bromoalkoxy)-3-(4'-decyloxyphenyl)-4*H*-1-benzopyran-4-ones, Br-n-I (n = 3-12)**

**HDI** (0.50 g, 1.27 mmol) was mixed with 3 equiv. of the corresponding dibromoalkane in acetone. 3 equiv. of potassium carbonate anhydrous was then added to the solution and the mixture was refluxed for 6 hours. The reaction mixture was cooled to room temperature and excess solvent was removed via evaporation. Water was then added to the mixture and the resulting precipitate was filtered and dried. The crude product was recrystallized from a solution of chloroform and ethanol (1:1, v/v).

#### **2.3.1.5 Syntheses of 7-[{4-[4'-((*S*)-2''-methylbutyloxy)carbonylphenyl]phenoxy}alkoxy]-3-(4'-decyloxyphenyl)-4*H*-1-benzopyran-4-ones, BP-n-I (n = 3-12)**

**Br-n-I** (0.30 g) and 1.2 equiv. of **HBP** were dissolved in acetone. 3 equiv. of potassium carbonate anhydrous was then added to the solution, together with a catalytic amount of potassium iodide and the reaction mixture was refluxed for 12 hours. The reaction mixture was cooled to room temperature and excess solvent was removed via evaporation. Water was then added to the mixture and resulting precipitate filtered, washed with acetone and recrystallized from a solution of chloroform and ethanol (1:1, v/v).

### 2.3.2 Preparation of 7-[{4-[4'-((*S*)-2''-methylbutyloxy)carbonylphenyl]phenoxy}decyloxy]-3-(4'-substitutedphenyl)-4*H*-1-benzopyran-4-ones, **BPI-R** (R = H, CH<sub>3</sub>, OCH<sub>3</sub>, F, Cl, Br)

The aforementioned were synthesized according to the synthetic routes shown in Figure 2.2.

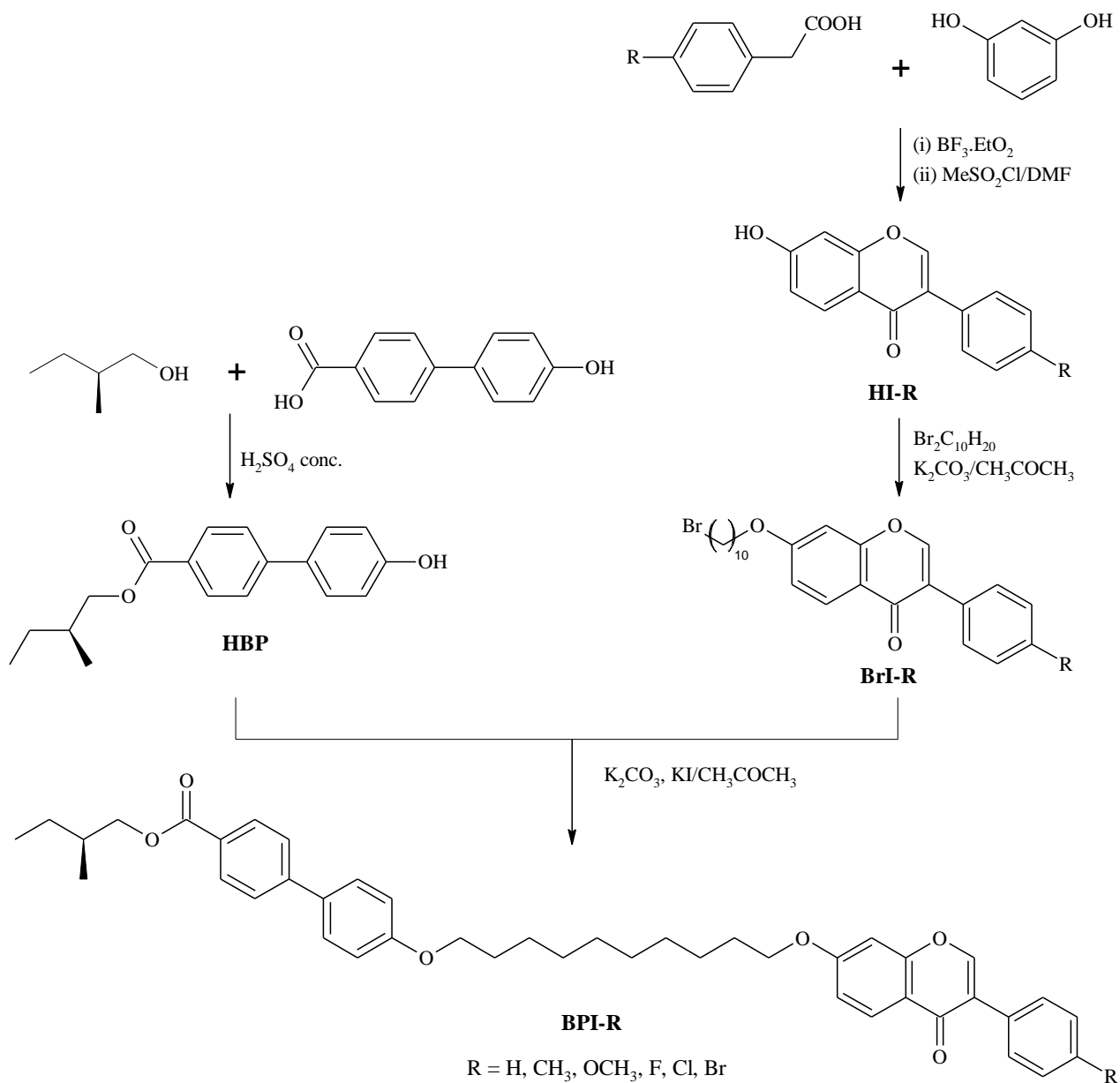


Figure 2.2: Synthetic scheme for the formation of 7-[{4-[4'-((*S*)-2''-methylbutyloxy)carbonylphenyl]phenoxy}decyloxy]-3-(4'-substitutedphenyl)-4*H*-1-benzopyran-4-ones, **BPI-R**.

**2.3.2.1 Syntheses of 7-hydroxy-3-(4'-substitutedphenyl)-4*H*-1-benzopyran-4-ones, **HI-R** (R = H, CH<sub>3</sub>, OCH<sub>3</sub>, F, Cl, Br)**

**HI-R** were synthesized using a similar method as described in Section 2.3.1.3, wherein 4-decyloxyphenylacetic acid was replaced by phenylacetic acid, 4-methylphenylacetic acid, 4-methoxyphenylacetic acid, 4-fluorophenylacetic acid, 4-chlorophenylacetic acid and 4-bromophenylacetic acid.

**2.3.2.2 Syntheses of 7-(10-bromodecyloxy)-3-(4'-substitutedphenyl)-4*H*-1-benzopyran-4-ones, **BrI-R** (R = H, CH<sub>3</sub>, OCH<sub>3</sub>, F, Cl, Br)**

**BrI-R** were synthesized using a similar method as described in Section 2.3.1.4, wherein **HDI** was replaced by the corresponding **HI-R** and 1,10-dibromodecane.

**2.3.2.3 Syntheses of 7-[[4-[4'-((*S*)-2''-methylbutyloxy)carbonylphenyl]phenoxy} decyloxy]-3-(4'-substitutedphenyl)-4*H*-1-benzopyran-4-ones, **BPI-R** (R = H, CH<sub>3</sub>, OCH<sub>3</sub>, F, Cl, Br)**

**BPI-R** were synthesized according to the method as described for Section 2.3.1.5, wherein **Br-n-I** was replaced by the corresponding **BrI-R**.

### 2.3.3 Preparation of 7-[{4-[(4'-methoxyphenyl)diazenyl]phenoxy}alkyloxy]-3-(4'-methoxyphenyl)-4*H*-1-benzopyran-4-ones, AB-*n*-I (n = 3-10)

The aforementioned were synthesized according to the synthetic routes shown in Figure 2.3.

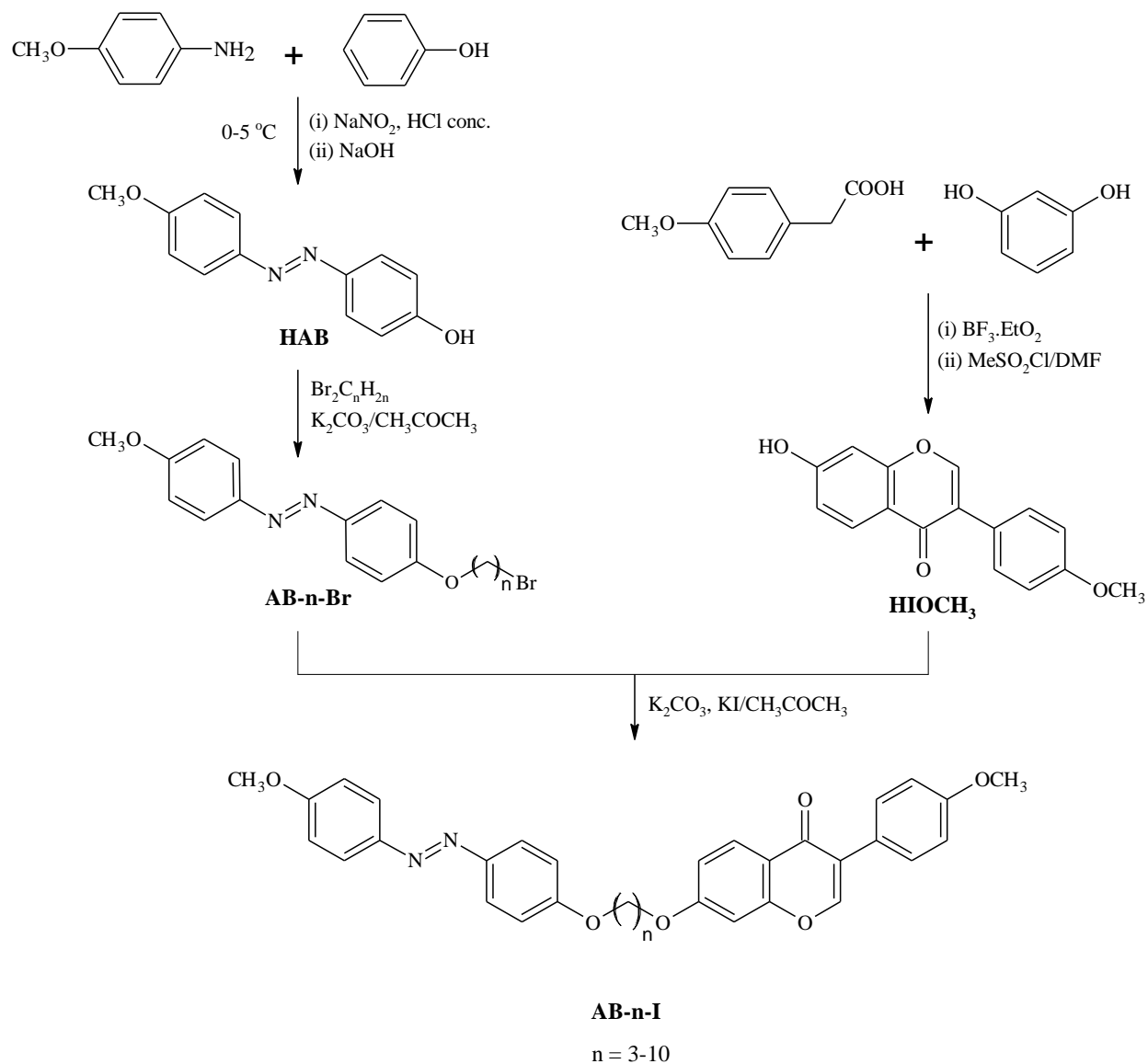


Figure 2.3: Synthetic scheme for the formation of 7-[{4-[(4'-methoxyphenyl)diazenyl]phenoxy}alkyloxy]-3-(4'-methoxyphenyl)-4*H*-1-benzopyran-4-ones, AB-*n*-I.

### 2.3.3.1 Synthesis of 4-[(4'-methoxyphenyl)diazenyl]phenol, **HAB**

**HAB** was synthesized by adding an aqueous solution of sodium nitrite to a mixture of 4-methoxyaniline in concentrated hydrochloric acid, wherein the temperature of the mixture was kept within 0-5 °C. The cold mixture was then added dropwise to a cold mixture containing phenol, sodium hydroxide and water. Precipitate resulted from the acidification with aqueous hydrochloric acid was filtered and dried before recrystallized from acetone.

### 2.3.3.2 Syntheses of 1-[4-(n-bromoalkoxy)phenyl]-2-(4'-methoxyphenyl) diazene, **AB-n-Br** (n = 3-10)

3 equiv. of potassium carbonate anhydrous was added to a solution containing **HAB** (0.5 g, 2.19 mmol) and 3 equiv. of the corresponding dibromoalkanes in acetone. The mixture was then refluxed for 6 hours. The reaction mixture was cooled to room temperature and excess solvent was removed via evaporation. Water was then added to the mixture and the resulting precipitate was filtered and dried. The crude product was purified by column chromatography using dichloromethane as eluent.

### 2.3.3.3 Synthesis of 7-hydroxy-3-(4'-methoxyphenyl)-4*H*-1-benzopyran-4-one, **HI-OCH<sub>3</sub>**

**HI-OCH<sub>3</sub>** was synthesized using a similar method as described in Section 2.3.1.3, wherein 4-decyloxyphenylacetic acid was replaced by 4-methoxyphenylacetic acid.



#### 2.3.3.4 Syntheses of 7-[[4-[(4'-methoxyphenyl)diazenyl]phenoxy]alkyloxy]-3-(4'-methoxyphenyl)-4*H*-1-benzopyran-4-ones, AB-*n*-I (*n* = 3-10)

3 equiv. of potassium carbonate anhydrous was added to a mixture of **HIOCH<sub>3</sub>** (0.3 g, 1.12 mmol) and 0.83 equiv. of **AB-*n*-Br** in acetone. A catalytic amount of potassium iodide was then added and the reaction mixture was refluxed for 12 hours. The reaction mixture was cooled to room temperature and excess solvent was removed via evaporation. Water was then added to the mixture in order to remove the potassium carbonate and potassium iodide. The resulting precipitate was filtered, washed using acetone and recrystallized from a solution of chloroform and ethanol (1:1, v/v).